Microelectronic Engineering 260 (2022) 111795

Contents lists available at ScienceDirect

Microelectronic Engineering

journal homepage: www.elsevier.com/locate/mee

Organotin bearing polymeric resists for electron beam lithography

Midathala Yogesh [a,1], Mohamad G. Moinuddin [b,1], Lalit D. Khillare [a], Srinivas Chinthalapalli [c], Satinder K. Sharma [b], Subrata Ghosh [a,*], Kenneth E. Gonsalves [a,*]

[a] School of Basic Sciences, Indian Institute of Technology Mandi, H.P. 175005, India
[b] School of Computing and Electrical Engineering, Indian Institute of Technology Mandi, H.P. 175005, India.
[c] Analytical and Spectroscopy Division, PCM Entity, Vikram Sarabhai Space Centre, Thiruvananthapuram 695022, India.

ARTICLE INFO

Keywords:
Functional polymer
Organotin
Organic-inorganic hybrid resist
Electron beam lithography
Nanopatterning

ABSTRACT

In recent time, inorganic and organic-inorganic hybrid resists are gaining considerable attention of resist community as the presence of inorganic component helps in improving many properties. The present work reports the development of an organotin bearing functional polymeric positive tone resist (**FPPTR-1**) comprised of rationally chosen four monomeric units viz. triphenylsulfonium salt 4-(methacryloxy) 2,3,5,6-tetrafluorobenzenesulfonate (F4-MBS-TPS), tertiary butyl acrylate (TBAC), γ-butyrolactone methacrylate (GBLMA) and acetoxydibutyltin methacrylate (ADBTMA). The resulting polymer was characterized using Nuclear Magnetic Resonance (NMR) spectroscopy, gel permeation chromatography (GPC), Fourier Transform Infrared (FT-IR) spectroscopy, X-ray photoelectron spectroscopy (XPS) and thermogravimetric analysis (TGA) techniques. The polymer has good thermal stability (~195 °C), and weight average molecular weight (Mw) was found to be ~9480. AFM studies revealed that the present functional polymer can form smooth film with low roughness. It showed good sensitivity to electron beam exposure (83 μC/cm^2). It was established through electron beam lithography (EBL) studies that **FPPTR-1** can be used as thermally stable positive tone e-beam resist with good contrast (~9.87) and sensitivity for nanopatterning of both thin (~30 nm) and relatively thick (~100 nm) film applications. We successfully patterned dense, isolated and complex nanofeatures using EBL.

1. Introduction

Since the realization of the potential of organometallic species, literature has witnessed development of large varieties of organometallic materials as well as strategies for inclusion of organometallic functionalities into molecular or macromolecular scaffolds for specific applications [1,2]. In the area of resist materials, organic photoresists particularly the chemically amplified photoresists (CARs) have been the workhorses for electronic chip fabrication in semiconductor industries [3–8]. With the advancement of electronic devices for better performance, the resolution of patterned features is becoming very critical [9]. For achieving good patterns at 30 nm regime, the thickness of the resist films are expected to be less than 35 nm in order to avoid high aspect ratio [10–12]. This is where the organic resists are confronting major challenges as the patterns of organic resists generated from a very thin film may fail to tolerate dry etching conditions [10,11]. In this regard, pure inorganic or organic-inorganic hybrid resists are anticipated to be the most promising patterning materials for future electronics fabrication [10,11,13–17]. Similarly, contrast of a resist is an important aspect as high contrast resists are the most desired ones [18,19]. The slope of normalized resist thickness (NRT) curve acts as an indicator of contrast of that particular resist.

While extreme ultraviolet lithography (EUVL) has emerged as highly advanced nanopatterning technique for high-volume manufacturing (HVM), [9–11,20–25] EBL has been a choice of lithography tool for specialized applications including optoelectronic devices, quantum structures, metamaterials, photomask fabrication, etc. [19,26–41]. Moreover, EBL is routinely used as a preferred lithography tool for academic research and development. Together, the importance of EBL and hence the resist compositions for EBL are quite evident.

In continuation of our interest in designing and developing new organometallic polymers as resist materials, [42] we report here the development of an organometallic polymer (**FPPTR-1**) bearing functional organotin as pendant group and its application as positive tone

* Corresponding authors.
E-mail addresses: subrata@iitmandi.ac.in (S. Ghosh), kenneth@iitmandi.ac.in (K.E. Gonsalves).
[1] Both authors have equal contribution

https://doi.org/10.1016/j.mee.2022.111795
Received 23 February 2022; Received in revised form 17 April 2022; Accepted 25 April 2022
Available online 29 April 2022

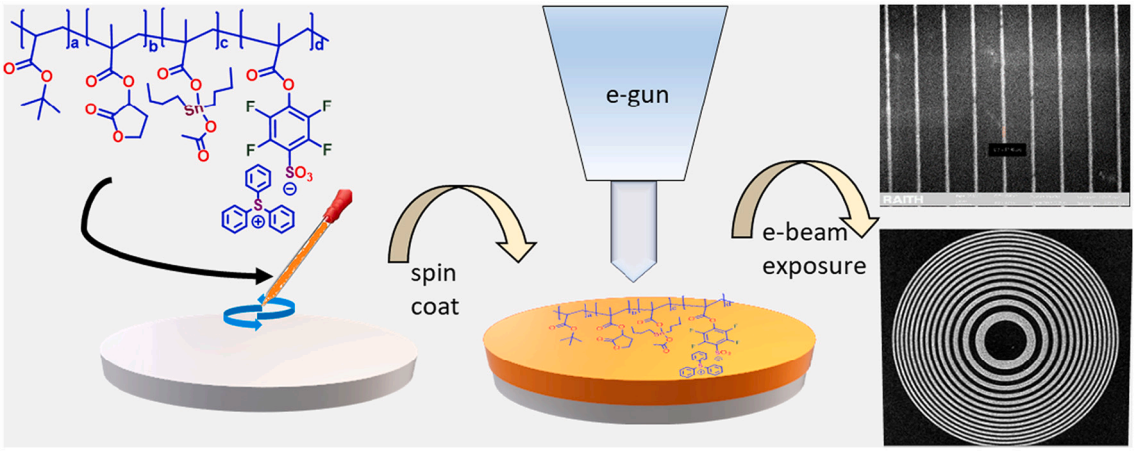

Scheme 1. Schematic on the development and application of **FPPTR-1**

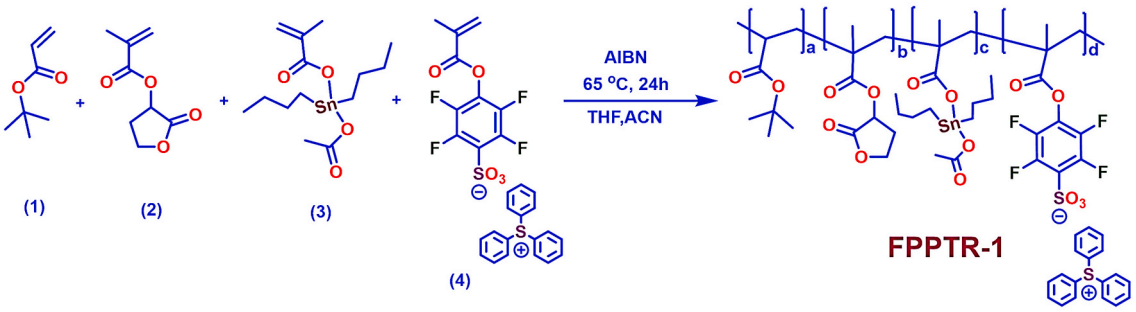

Scheme 2. Synthetic route for **FPPTR-1**

resist for nanopatterning using electron beam lithography (EBL) (Scheme 1). Among various inorganic and organic-inorganic resist materials, tin-based resist materials are gaining special attention. [9–11,20–22] The present tetrapolymer **FPPTR-1** comprises of triphenylsulfonium salt 4-(methacryloxy) 2,3,5,6-tetrafluorobenzenesulfonate (F4-MBS-TPS), tertiary butyl acrylate (TBAC), γ-butyrolactone methacrylate (GBLMA) and acetoxydibutyltin methacrylate (ADBTMA) as monomeric units (Scheme 2). The polymer was characterized by nuclear magnetic resonance (NMR) spectroscopy, Fourier transform infrared (FT-IR) spectroscopy, gel permeation chromatography (GPC), and thermogravimetric analysis (TGA). Our preliminary studies on EBL revealed that **FPPTR-1** can be used as a good contrast positive tone e-beam resist for sub-35 nm patterning.

The improvement in performance of polymeric resist compositions is generally achieved through polymer-structure engineering leading to development of multi-functional resists. In this regard, the monomer selection is done with a clear rationale as the monomers in a polymer network often control the desired properties. In general, the most desired properties of a resist composition include good adhesion with the patterning surface, resolution, etch resistance, polarity switching, sensitivity, contrast, wall profile, and so on. Hence, many properties can be integrated into a single polymeric network through incorporation of different monomers with specific roles. We paid special attention to monomer selection while designing the tetrapolymer as one of the target applications of this polymer is to use it as resist material. In brief, the F4-MBS-TPS unit (photoacid generator, PAG) was incorporated for solid state acid generation, GBLMA as adhesion promoter, ADBTMA (organometallic unit) as sensitivity, resolution, thermal property enhancer, and TBAC as polarity switching unit.

A detailed mechanistic study on a covalently bonded organotin-based resist through monochromatic synchrotron radiation irradiation at 103.5 eV followed by XPS, NEXAFS and theoretical calculations established that the incorporation of organotin functionality to the main polymer structure may lead to improved sensitivity and resolution of the resist [42]. Moreover, this report also shaded light on the importance of linking heavy metals through covalent bond with the polymer structure instead of their incorporation through electrostatic interaction [42]. Also, incorporation of heavy metal may lead to enhanced thermal stability of the resist. Therefore, in the current work, the ADBTMA functionality was incorporated into the main polymer structure to enhance overall performance of the developed resists.

2. Experimental section

2.1. Chemicals and reagents

Triphenylsulphonium chloride, triethylamine (TEA), trifluoro acetic anhydride, and trifluoro acetic acid were purchased from Sigma-Aldrich. α-Hydroxy-γ-butyrolactone and tertiary butyl acrylate (TBAC) were purchased from TCI India. AIBN (Azobisisobutyronitrile) was purchased from Avra Synthesis Private Limited and it was recrystallized two times before using for polymerization. Acetonitrile (ACN) was dried using calcium hydride (CaH_2) and tetrahydrofuran (THF) was dried using Na/benzophenone. The compounds γ-butyrolactone methacrylate (GBLMA), triphenylsulphonium salt 4-(methacryloxy)-2, 3, 5, 6-tetrafluorobenzenesulfonate (F4-MBS-TPS), and acetoxydibutyltinmethacrylate (ADBTMA) were synthesized following literature procedure and characterized using spectroscopic techniques [43–47].

2.2. Analytical measurements

NMR studies were performed on a Jeol JNM ECX 500 MHz spectrometer in $CDCl_3$ or DMSO-d_6 and TMS as internal standard. FTIR

Table 1
Polymerization conditions and other details of synthesized polymers.

Polymer/resist	Mole Feed Ratio				Microstructure Mole (%)				Yield (%)	Sn[a]Wt.(%)	Mw/Mn[b]	PDI[c]	T_d^d(°C)
	TBAC	GBLMA	ADBTMA	F4-MBS-TPS	TBAC	GBLMA	ADBTMA	F4-MB-TPS					
FPPTR-1	72	20	4	4	60.0	27.0	5.0	8.0	60	3.23	9480/5280	1.7	196

Sn[a] Wt% was calculated using ICP-OES. $M_{W/}Mn^b$ and PDI[c] were determined using polystyrene as a standard and THF as a solvent (the first place of Mw and Mn has been rounded off). T_d^d was measured at a heating rate of 10 °C/min in N_2.

spectrum was recorded on a PerkinElmer spectrum-2 spectrophotometer. Thermo gravimetric analysis (TGA) measurements were done on NETZSCH STA 449 F1 JUPITER Series instrument. The heating range was 10 °C /min in N_2 atmosphere over temperature range from 10 °C to 700 °C. GPC analysis was done with PL gel MIXED C 10 μm column using Agilent Technologies, 1260 Infinity Series instrument. The molecular weight of the polymer was calculated with respect to polystyrene as narrow Mw standards and THF was used as the eluent.

3. Synthesis

3.1. Synthetic procedure for FPPTR-1

In 50 mL schlenk flask TBAC (**1**) (1.37 g, 10.73 mmol), GBLMA (**2**) (0.5 g, 2.94 mmol), ADBTMA (**3**) (0.22 g, 0.58 mmol), F4-MBS-TPS (**4**) (0.33 g, 0.58 mmol) and AIBN (0.8%) were dissolved in a mixture of dry acetonitrile/tetrahydrofuran (1:2 *v*/v) under N_2 atmosphere. The reaction mixture was degassed by N_2 gas. Subsequently, the reaction mixture was stirred at 65 °C under N_2 atmosphere for 24 h. After that, the reaction mixture was cooled to room temperature and precipitated out in n-hexane (50 mL). The resulting solid product was filtered and dried in a temperature-controlled oven at 50 °C for 24 h.Yield: 1.47 g. FT-IR: $\nu_{max/}cm^{-1}$ 2976, 2927 (CH), 1786 (C=O), 1247 (C—F), 530 (Sn—C). ^{1}H NMR (500 MHz, DMSO-d_6, δ): δ_H 7.07–8.20 (15H, br, ArH), 5.13–5.69 (1H, br, GBLMA unit), 3.93–4.72 (2H, br, GBLMA unit), 0.19–2.67 (aliphatic).

4. Results & discussion

An organometallic tetrapolymer (**FPPTR-1**), based on F4-MBS-TPS, ADBTMA, TBAC and GBLMA monomeric units, was synthesized using different molar feed ratio of monomers (see Scheme 2 and Table 1) in the presence of the AIBN, and a mixture of ACN and THF (1:2) as solvent at 65 °C under N_2 atmosphere for 24 h. After that, the polymer was precipitated in hexane to obtain final product as a white powder. While synthesizing the polymer, we observed some sort of insolubility of the end product when polymerization was done in THF alone. However, use of mixed solvent improved the solubility resulting in effective polymerization. The tetrapolymer thus obtained was characterized using various analytical techniques such as FTIR, NMR, GPC, XPS, and TGA. Fig. S1 represents the ^{1}H NMR spectra of **FPPTR-1** and Fig. S2 represents the stacked ^{1}H NMR spectra of all respective monomers and polymer. The broad peaks at 7.07–8.20 are assigned to cationic triphenylsulphonium functionality, the peaks at 3.93–4.72 are due to -OCH_2 protons of γ-butyrolactone, and the peak at 5.13–5.69 is due to -OCH proton of γ-butyrolactone. Moreover, the presence of broad peak at 0.19–2.67

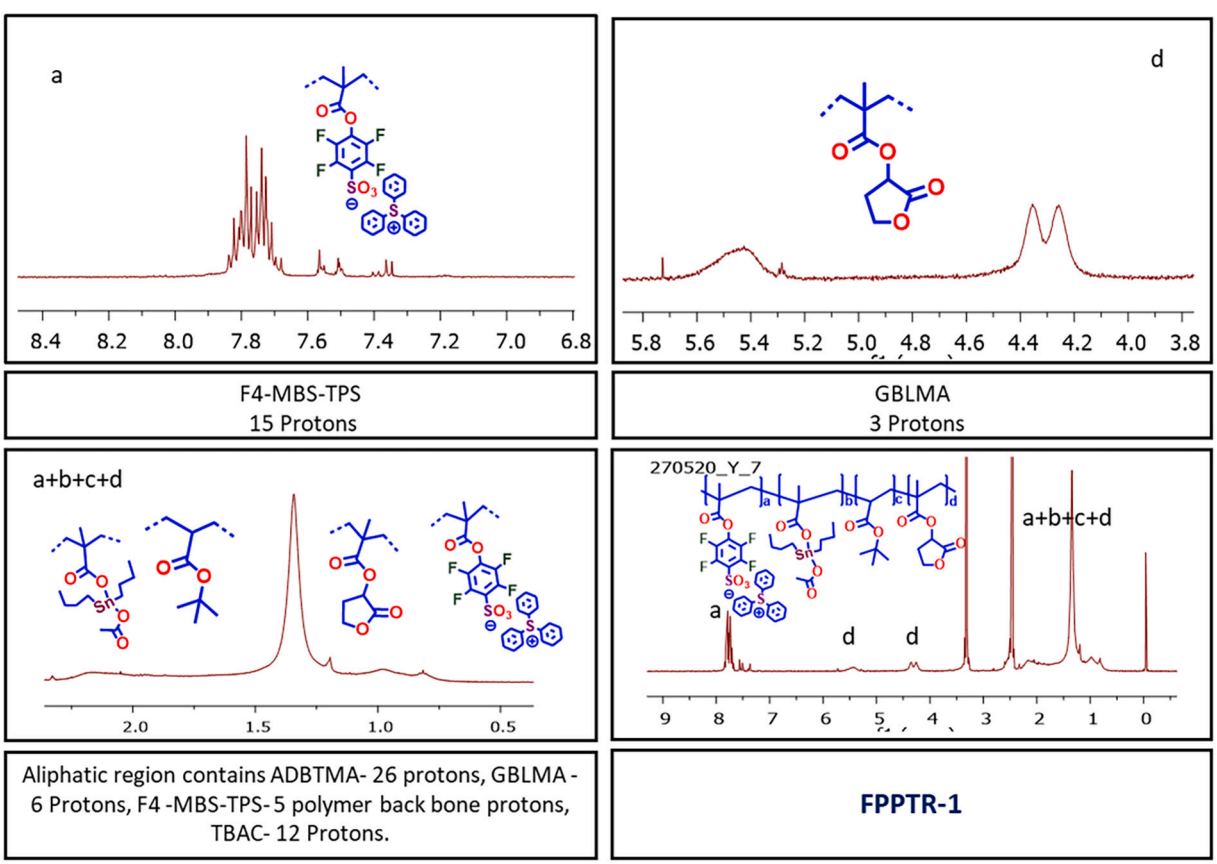

Fig. 1. Microstructure calculation for **FPPTR-1** using ^{1}H NMR.

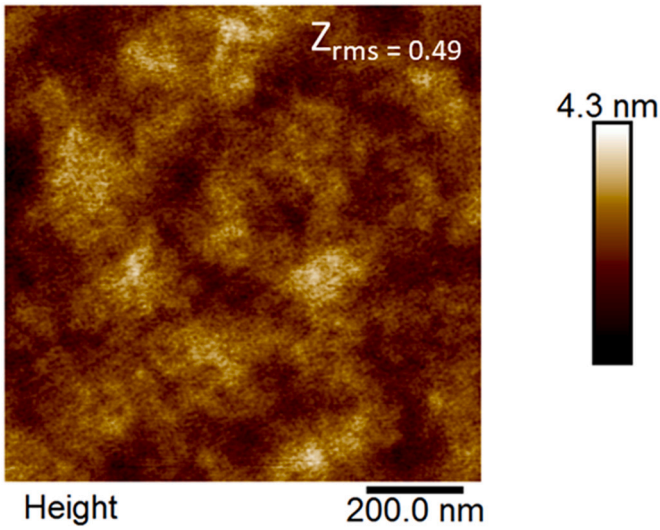

Fig. 2. AFM surface morphology studies of tetrapolymer **FPPTR-1**.

ppm is due to -CH_3 and-CH_2 protons of the polymer chain and aliphatic functionalities. The disappearance of olefinic proton peaks supported polymerization of monomers.

FT-IR spectra of **FPPTR-1** exhibiting absorption bands at 2976 and 2927 cm^{-1} are due to CH stretching frequencies (**Fig. S3**). The stretching vibration of carbonyl group present in the polymer chain was observed at 1786 cm^{-1}. Absorption bands observed at 1247 and 530 cm^{-1} indicate the presence of C—F and Sn—C functionalities [48,49] which further support the presence of F4-MBS- TPS and ADBTMA moieties in the polymer chain.

The weight average molecular weight (M_w) and number average molecular weight (M_n) of **FPPTR-1** were calculated using gel permeation chromatography (GPC). For this study, PL gel mixed-C with pore size 10 μm was used as column compartment and THF was used as eluent at 1 mL/min flow rate at 35 °C. Polystyrenes were used as standards to plot GPC graph for analysis of M_w. The calculated M_w and M_n of **FPPTR-1** was found to be ~9480 and ~5280, and the polydispersity index (PDI) was found to be 1.7 (see **Fig. S4**, Table 1).

Thermal stability of **FPPTR-1** was evaluated through the thermogravimetric analysis (TGA) (see Table 1). The TGA graph of **FPPTR-1** shows that the T_d of **FPPTR-1** is ~195 °C (**Fig. S5**). This value indicates that **FPPTR-1** has good thermal stability.

Next, to get an idea about the presence of tin in polymer network, XPS analyses were performed. The XPS data clearly indicated the presence of tin in polymer matrix (**Fig. S6**). Elemental analyses were performed to evaluate tin percentage in polymer matrix (**Fig. S7**). To estimate microstructure percentage in FPPTR-1, initially the weight percentage of tin monomer was calculated using the tin content data obtained from ICP-OES analysis. The mole percentages of the four monomers in polymer were obtained from ^{1}H NMR spectra with the help of weight percentage obtained from ICP-OES analysis (see 'Microstructure calculation' in ESI for details). The microstructure composition calculation using a combination of elemental analysis and ^{1}H NMR results revealed incorporation of ~27% GBLMA, ~60% TBAC, ~5% ADBTMA and ~ 8% F4-MBSTPS into the polymer network of FPPTR-1 (Fig. 1).

After complete characterization of **FPPTR-1**, we started focusing on its application. The solubility of **FPPTR-1** in different solvent was studied, and we found that **FPPTR-1** has good solubility in DMAC (**Table S1**). Initially, 3 wt% solution in dimethylacetamide (DMAC) was prepared and spin coated on a (2 × 2 cm^2) silicon wafer to obtain film thickness of ~30 nm (**Fig. S8**). After spin coating, the film was baked at 130 °C for one minute to get a dry film. Then, the tin doped film uniformity was analysed using atomic force microscope (AFM) integrated with a antimony doped silicon (cantilever) tip (Bruker, USA) with a radius of curvature 7–10 nm and spring (force) constant of the cantilever 42 N/m and utilized for polymeric thin films topography analysis. As evident from the AFM analysed surface image (Fig. 2), **FPPTR-1** formed uniform thin film with computed average surface roughness (Rq) of 0.49 nm. The RMS value was taken in 512 pixels in 1 × 1 μm^2 scanning area and this Rq value was found to be almost minimal for ~30 nm resist film, an important parameter for lithographic application as shown in Fig. 2.

Also, as spin speed versus thickness is an important parameter for optimization of resists film with desired thickness, we established a correlation between spin speed (rpm) and thickness of resist with different solid loading in the solution, viz. 3, 5 and 8 wt% of **FPPTR-1** in DMAC (**Fig. S9**). Finally, EBL studies were conducted with **FPPTR-1** to check its sensitivity toward electron beam. The resist was found to be sensitive to 83 μC/cm^2 dose (E_0) under electron beam with a contrast (λ) of ~9.87 ($\lambda = \left(log\frac{D_{90}}{D_{10}}\right)^{-1}$ where D_x are the doses with x% thickness loss, as evaluated from the NRT curve (Fig. 3). Hence, one can expect nanoscale patterning using this resist formulation by EBL. The NRT curve was established by exposing the resist film at different doses followed by measuring the remaining thickness of the resist film after developing, and then plotting the remaining thickness with respect to

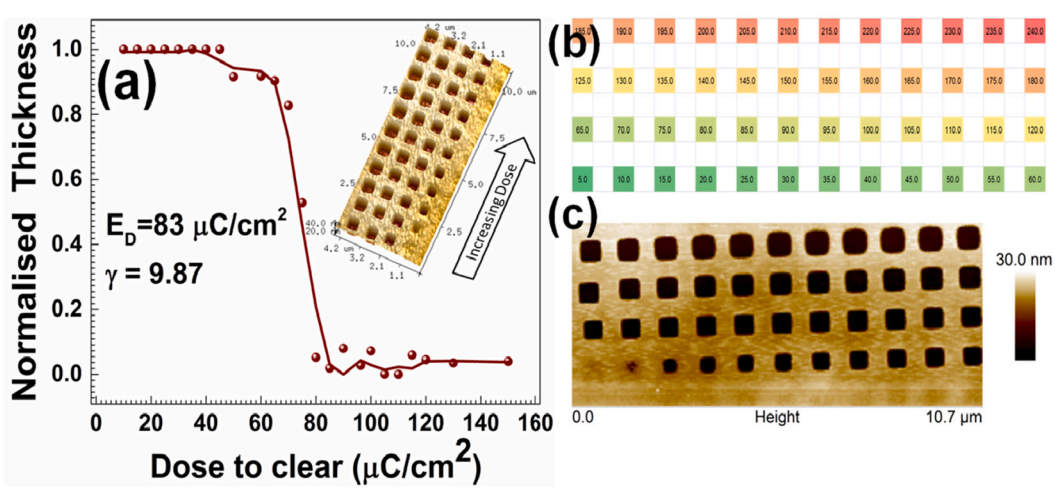

Fig. 3. (a) Sensitivity contrast curve (NRT) of resist **FPPTR-1** showing good contrast of 9.87; (b) schematic of variable dose analysis under EBL (20 keV) with exposure dose step of 5 μC/cm^2; (c) atomic force micrograph of exposed films with varied doses.

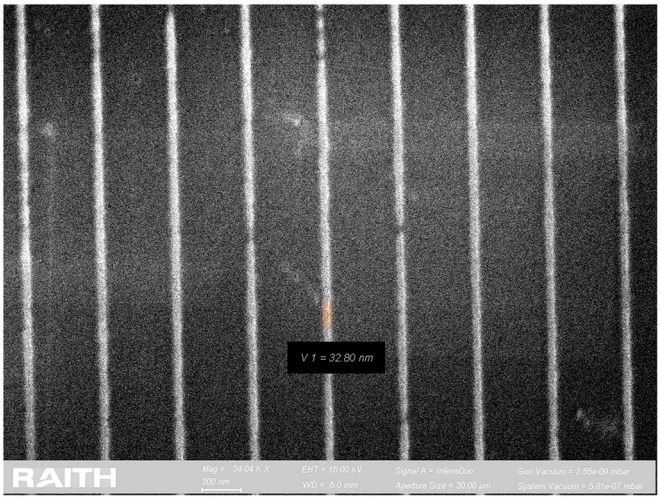

Fig. 4. SEM micrographs of ~33 nm patterns of the positive tone resist **FPPTR-1** (thickness ~30 nm).

dose. The sharp NRT curve indicates good contrast of this resist. It is to be pointed out that the present hybrid system showed good sensitivity.

For EBL, 3.0 wt% resist solution was prepared by dissolving **FPPTR-1** in dimethylacetamide (DMAC). The solution was double filtered through 0.2 μm teflon filter to remove any particles present in the resist solution, and then the filtered resist was spin coated on the 2″ p-type RCA cleaned silicon wafers at a speed of 6000 rpm for 90 s to obtain the thickness of ~30 nm. These films are pre-baked at 130 °C using hot plate to remove the residual solvent from the coated resist. The coated films were exposed using 20 KeV e-beam energy under EBL (e-Line PLUS). After exposure, the resist thin film was post-baked at 130 °C for 60 s on a hot plate. The exposed samples were developed in 0.026 N tetramethyl ammonium hydroxide (TMAH) solution for 25 s, rinsed with DI water for 30 s and dried using nitrogen gas. During developing in TMAH solution, the exposed region of resist material got dissolved away and the unexposed region remained undissolved resulting in the formation of positive tone patterns which possibly due to suitable change in the polarity of the resist material during exposure and postbake. The EBL results of **FPPTR-1** showed line pattern resolution up to ~33 nm width at a dose of 160 μC cm^{-2} (Fig. 4) and ~50 nm dense (L/S) patterns at a dose of 100 μC cm^{-2} (**Fig. S10**). One of the critical parameters for nanopatterns is their line-width roughness (LWR) for practical applications. The LER of ~55 nm patterns was found to be 3.60 nm (**Fig. S11**) which is less than 10% of the feature size, this further possibly establishes the possible application of the present resist [50,51].

Given the importance of complex features in fabricating electronic devices such as photonic, NEMS/MEMS etc. devices, we tested the potential of **FPPTR-1** as resist material for patterning complex features using EBL. We successfully patterned round-shaped complex features of various size (Fig. 5) which were characterized using FE-SEM and AFM techniques. Finally, and to widen the scope of application of the current resist system, we investigated the patterning of relatively thick film of ~100 nm thickness (**Fig. S12**). We could print ~90 nm patterns with line/space features at a dose of 85 μC cm^{-2} (Fig. 5). For thick film patterning, the resist solution was prepared by dissolving 8 wt% resist (**FPPTR-1**) in DMAC and the solution was double filtered through 0.2 μm Teflon filter. The filtered solution was spin-coated at 4000–6000 rpm on a RCA cleaned silicon wafer followed by prebake at 130 °C on a hot plate for 60 s. The coated films were subjected to EBL followed by a postbake at 130 °C, developed in 0.026 N TMAH solution for 50 s, rinsed

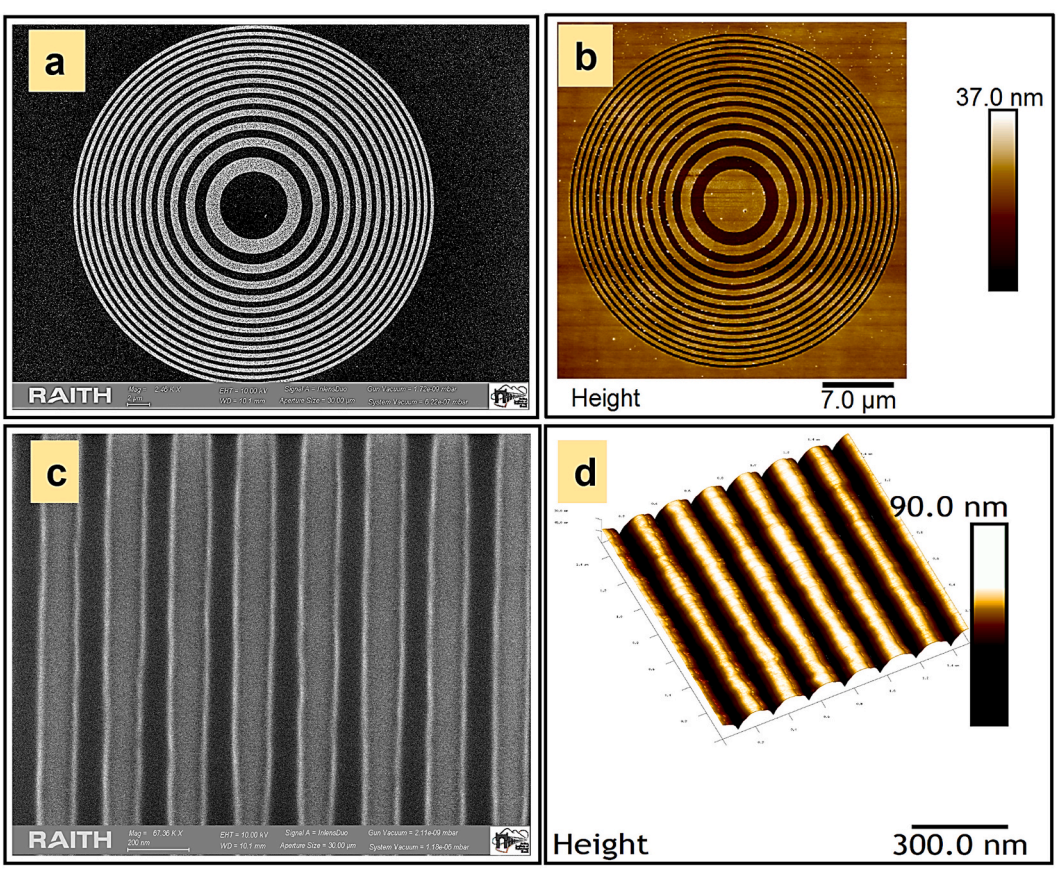

Fig. 5. High resolution micrographs of the complex features of **FPPTR-1**: (a) FESEM image of features ranging from ~120 nm - 1 μm; (b) AFM image of the same patterns. (c) ~90 nm L/S patterns of thick film of **FPPTR-1**; (d) AFM image of same patterns.

Table 2
Lithography performance of reported e-beam resists and the current resist.

Resist	Sensitivity ($\mu C/cm^2$)	Contrast	Resolution (nm)	Tone	Family	Developer	Voltage (kV)	Ref
L SU-8	*~20*	*0.8*	*~24*	*Neg*	*CAR*	PGMEA	100	[52]
CSAR 62	*55 (D_o)*	*~14*	*~7*	*Pos*	*CAR*	X AR 600–54/6	30	[53]
HN 409	*8–24*	–	*50–100*	*Neg*	*CAR*	MF702	50	[54]
HN 432	*26–126*		30–100				50	[54]
FEVS	*~18* (mC/cm^2)	–	*~20*	–	*CAR*	TMAH	50	[55]
PMMA	5.8 (mC/cm^2)	4	*5–10*	Neg	*n-CAR*	MIBK/IPA	2–30	[56]
	325 (PMMA coated with a thin layer of evaporated Cr)		4	Pos	*n-CAR*	Water: IPA	30	[57]
HSQ	*500–3000*	*3–10*	*4.5*	*Neg*	*n-CAR*	TMAH, 1 wt% NaOH and 1 wt% NaOH, 4 wt% NaCl	10	[58]
ZEP 7000	*~60–180*		*~12–15*	*Pos*	*n-CAR*	Hexyl acetate	25	[59]
ZEP	*~80*	*~25*	*~11*	*Pos*	*n-car*	Amyl acetate	20	[60]
poly (GMA-*co*- MMA-co-TPSMA	*120*	–	*15*	*Neg*	*CAR*	7:3 IPA: DI water	100	[5]
poly (MAPDST-*co*-ADSM)	200	*2.54*	*12.3*	*Neg*	*n-CAR*	TMAH	20	[61]
SML	107	*12*	*~15*	*Pos*	*Methacrylate*	IPA: DI water	10	[62]
HafSOx	21 ($D_{0.8}$)	*2.5*	*9* [63]	*Neg*	*Inorganic*	TMAH	10	[63,64]
ZircSOx	7.6 ($D_{0.8}$)	*2.6*	*15*	*Neg*	*Inorganic*	TMAH	30	[64]
40XT in combination with PEDOT: PSS	<10	*~10*	*~85*	*Pos*	*CAR*	AZ7 26mif	20	[65]
P(HEMA-co-MAAEMA)	0.5	*1.2*	*100–200*	*Neg*	*n-CAR*	Methanol	50	[37]
C60-(P(CMS14-HS))	–	–	*50*	*Neg*	*Fullerene derivative*	Acetone	100	[66]
IM-MFPT12–8	43	*1.3*	*13.6*	*Neg*	*CAR*	MCB: IPA	20	[67]
Mr-Pos EBR (Copolymer)	74	*~4*	*29*	*Pos*	*Methacrylate*	Amyl acetate	30	[68]
Sodium PSS	2800	*0.8*	*40*	*Neg*	–	Water	20	[69]
MoS_2	34–57	*3.3–5.1*	*9*	*Neg*	–	Chloroform	100	[70]
Zinc Alkylxanthate	26–46	*1.8–11.2*	*6*	*Neg*	Metal xanthates	Chloroform	100	[71]
Silk	2250 (positive) 25,000(Negative)	–	*30*	*Pos* *Neg*		Water	100	[72]
FPPTR-1	*83*	*9.87*	*~33*	*Pos*	*CAR*	TMAH	20	Present work

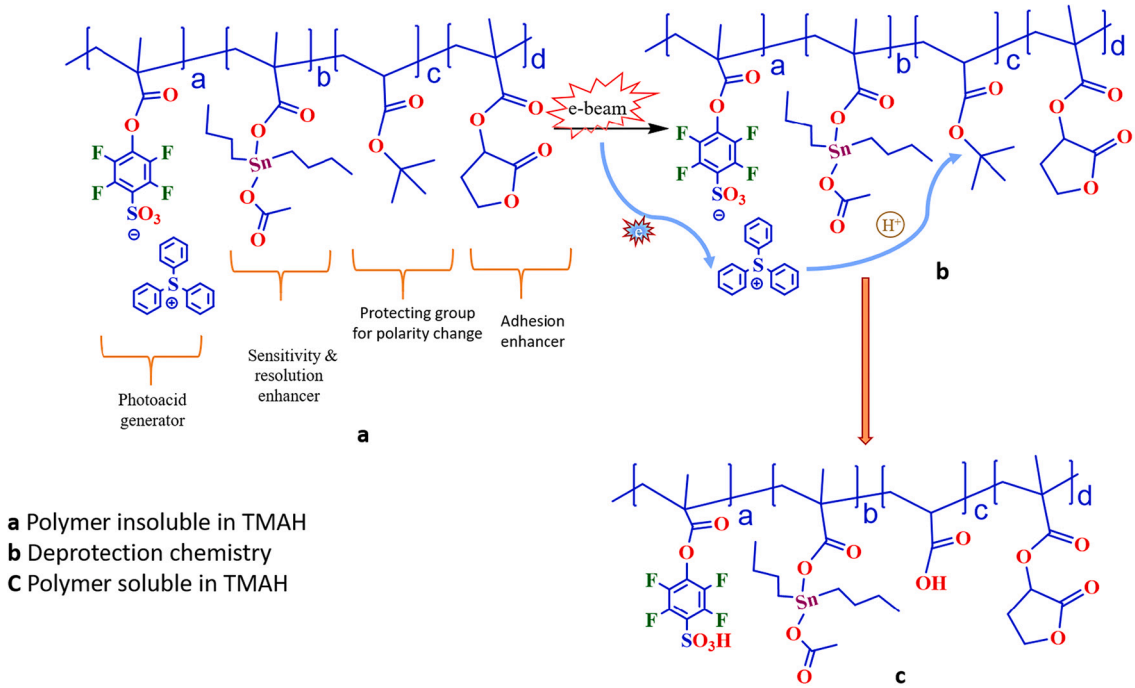

Scheme 3. Proposed mechanism for e-beam expoure triggered polarity switching

with DI water for 30 s and finally dried using nitrogen gas. The SEM image of ~90 nm L/S features with good pattern fidelity was supported by AFM measurements (Fig. 5). Table 2 provides a detailed comparison of the performance of the present resist system with the reported ones.

To shed light into a possible pathway for desired polarity switching after exposure and post bake, which in fact governs the patterning process, we propose that the photoacid generator F4-MBS TPS (PAG) present in the polymer chain liberates acid in solid state when the resist is exposed with e-beam [45,73]. As known in the literature, the sulfonium functionality liberates acids when exposed with photon or electron beam as it undergoes decomposition through a fragmentation process upon irradiation with photon or electron beam resulting in the generation of reactive proton (acid generation) [5,73–76]. As the present polymer contains sulfonium component as pendant group, we anticipate that it produces acid in the solid state when exposed with electron beam. The generated acid reacts with the TBAC to convert it to a carboxylic acid through deprotection chemistry [73]. This chemistry leads to polarity switching and makes the exposed polymer soluble in aqueous TMAH solution resulting in pattern development (Scheme 3).

5. Conclusion

Given the importance of resist materials with potential for forming film of thickness ~ 30 nm or less for nanopatterning, inorganic and organic-inorganic hybrid photoresists are being anticipated to have better potential for specialized applications. We report a functional organotin containing polymeric radiation sensitive material comprised of F4-MBS-TPS, TBAC, GBLMA and ADBTMA as monomeric units. Each monomer was chosen with a purpose keeping in mind the possible application of this polymer as resist material. While GBLMA was introduced to act as adhesion promoter during thin film formation on the coating surface, F4-MBS-TPS was incorporated as solid-state acid generator. The main objective behind the introduction of ADBTMA is to improve sensitivity, resolution, and thermal property, whereas TBAC acts as polarity switching unit during exposure and post-exposure baking conditions. The developed polymer was characterized using relevant analytical tools including GPC, NMR, FTIR and TGA. The polymer **FPPTR-1** was thermally stable up to ~195 °C. Finally, **FPPTR-1** showed good sensitivity toward electron beam and can be used as positive tone e-beam resist with good contrast (~9.87) and sensitivity (83 $\mu C/cm^2$). This resist printed well-developed ~33 nm line features as well as complex patterns. In addition to thin film application (thickness ~ 30 nm), we used **FPPTR-1** also for relatively thick film (thickness ~ 100 nm) dense patterning. As this resist has shown good sensitivity and contrast toward EBL, we anticipate that the same composition may possibly be used for EUVL application as EBL is often used as prescreening tool while developing new EUV resists.

Credit author satement

Midathala Yogesh: Synthesis, Characterization, Lithography, Data curation, Initial draft preparation; **Mohamad. G. Moinuddin**: Lithography, image analysis, Data curation, Writing; **Lalit D. Khillare**: Writing; **Srinivas Chinthalapalli**: NMR analysis and microstructure calculation; **Satinder K. Sharma**: Lithography, image analysis and supervision; **Subrata Ghosh**: Conceptualization, supervision and editing; **Kenneth E. Gonsalves**: Conceptualization, supervision and reviewing.

Declaration of Competing Interest

The authors declare that they have no known competing financial interests.

Acknowledgement

Financial support from Uchchatar Avishkar Yojana (UAY) (Grant No. IITMandi_005) is thankfully acknowledged. Instrument facility at AMRC and CFDFED, IIT Mandi is acknowledged. M. Yogesh thanks CSIR for research fellowship. MGM is supported under the "Visvesvaraya PhD Scheme" by MEiTY, India. We acknowledge Mr. Kumar Palit for his help during AFM measurements.

Appendix A. Supplementary data

Supplementary data to this article can be found online at https://doi.org/10.1016/j.mee.2022.111795.

References

[1] K.A. Williams, A.J. Boydston, C.W. Bielawski, Main-chain organometallic polymers: synthetic strategies, applications, and perspectives, Chem. Soc. Rev. 36 (2007) 729–744, https://doi.org/10.1039/B601574N.
[2] J. Zhang, K. Cao, X.S. Wang, B. Cui, Metal-carbonyl organometallic polymers, PFpP, as resists for high-resolution positive and negative electron beam lithography, Chem. Commun. 51 (2015) 17592–17595, https://doi.org/10.1039/c5cc07117h.
[3] D.K. Lee, G. Pawlowski, The frog prince - a brief review of DUV resist technology, J. Photopolym. Sci. Technol. 15 (2002) 427–434, https://doi.org/10.2494/photopolymer.15.427.
[4] D.P. Sanders, Advances in patterning materials for 193 nm immersion lithography, Chem. Rev. 110 (2010) 321–360, https://doi.org/10.1021/cr900244n.
[5] J.B. Yoo, S.W. Park, H.N. Kang, H.S. Mondkar, K. Sohn, H.M. Kim, K.B. Kim, H. Lee, Triphenylsulfonium salt methacrylate bound polymer resist for electron beam lithography, Polymer (Guildf). 55 (2014) 3599–3604, https://doi.org/10.1016/j.polymer.2014.06.008.
[6] C.S. Whelan, Low energy electron beam top surface image processing using chemically amplified AXT resist, J. Vacuum Sci. Technol. B: Microelectron Nanomet. Struct. 15 (1997) 2555, https://doi.org/10.1116/1.589684.
[7] S. Thoms, D.S. Macintyre, Investigation of CSAR 62, a new resist for electron beam lithography, J. Vacuum Sci. Technol. B, Nanotechnol. Microelectronics: Mater. Process. Measur. Phenomena. 32 (2014) 06FJ01, https://doi.org/10.1116/1.4899239.
[8] R.A. Lawson, C.T. Lee, W. Yueh, L. Tolbert, C.L. Henderson, Epoxide functionalized molecular resists for high resolution electron-beam lithography, Microelectron. Eng. 85 (2008) 959–962, https://doi.org/10.1016/j.mee.2008.01.080.
[9] L. Li, X. Liu, S. Pal, S. Wang, C.K. Ober, E.P. Giannelis, Extreme ultraviolet resist materials for sub-7 nm patterning, Chem. Soc. Rev. 46 (2017) 4855–4866, https://doi.org/10.1039/C7CS00080D.
[10] Z. Wang, X. Yao, H. An, Y. Wang, J. Chen, S. Wang, X. Guo, T. Yu, Y. Zeng, G. Yang, Y. Li, Recent advances in organic-inorganic hybrid photoresists, J. Microelectron. Manufact. 4 (2021) 1–8, https://doi.org/10.33079/jomm.21040101.
[11] C. Luo, C. Xu, L. Lv, H. Li, X. Huang, W. Liu, Review of recent advances in inorganic photoresists, RSC Adv. 10 (2020) 8385–8395, https://doi.org/10.1039/c9ra08977b.
[12] H. Tsubaki, S. Tarutani, H. Takizawa, T. Goto, EUV resist materials for 20nm and below half-pitch applications, Adv. Resist Mater. Process. Technol. XXIX. 8325 (2012), 832509, https://doi.org/10.1117/12.916378.
[13] Y. Wang, D. Astruc, A.S. Abd-El-Aziz, Metallopolymers for advanced sustainable applications, Chem. Soc. Rev. 48 (2019) 558–636.
[14] C. Acikgoz, M.A. Hempenius, J. Huskens, G.J. Vancso, Polymers in conventional and alternative lithography for the fabrication of nanostructures, Eur. Polym. J. 47 (2011) 2033–2052, https://doi.org/10.1016/j.eurpolymj.2011.07.025.
[15] T. Mpatzaka, G. Zisis, I. Raptis, V. Vamvakas, C. Kaiser, T. Mai, M. Schirmer, M. Gerngroß, G. Papageorgiou, Process study and the lithographic performance of commercially available silsesquioxane based electron sensitive resist medusa 82, Micro Nano Eng. 8 (2020), 100065, https://doi.org/10.1016/j.mne.2020.100065.
[16] M. Rohdenburg, N. Thakur, R. Cartaya, S. Castellanos, P. Swiderek, Role of low-energy electrons in the solubility switch of Zn-based oxocluster photoresist for extreme ultraviolet lithography, Phys. Chem. Chem. Phys. (2021), https://doi.org/10.1039/D1CP02334A.
[17] M.S.M. Saifullah, M. Asbahi, M. Binti-Kamran Kiyani, S. Tripathy, E.A.H. Ong, A. Ibn Saifullah, H.R. Tan, T. Dutta, R. Ganesan, S. Valiyaveettil, K.S.L. Chong, Direct patterning of zinc sulfide on a Sub-10 nanometer scale via Electron beam lithography, ACS Nano 11 (2017) 9920–9929, https://doi.org/10.1021/acsnano.7b03951.
[18] A. Kaganskiy, T. Heuser, R. Schmidt, S. Rodt, S. Reitzenstein, CSAR 62 as negative-tone resist for high-contrast e-beam lithography at temperatures between 4 K and room temperature, J. Vacuum Sci. Technol. B, Nanotechnol. Microelectronics: Mater. Process. Measur. Phenomena. 34 (2016), 061603, https://doi.org/10.1116/1.4965883.
[19] H. Duan, V.R. Manfrinato, J.K.W. Yang, D. Winston, B.M. Cord, K.K. Berggren, Metrology for electron-beam lithography and resist contrast at the sub-10 nm scale, J. Vacuum Sci. Technol. B, Nanotechnol. Microelectronics: Mater. Process. Measur. Phenomena. 28 (2010), https://doi.org/10.1116/1.3501359. C6H11-C6H17.
[20] K. Sakai, H. Xu, V. Kosma, E.P. Giannelis, C.K. Ober, Progress in metal organic cluster EUV photoresists, J. Vac. Sci. Technol. B 36 (2018) 06J504, https://doi.org/10.1116/1.5050942.

[21] H. Xu, V. Kosma, K. Sakai, E.P. Giannelis, C.K. Ober, EUV photolithography: resist progress in metal–organic complex photoresists, J. Micro/Nanolithogr MEMS MOEMS. 18 (2018) 1–10, https://doi.org/10.1117/1.JMM.18.1.011007.

[22] J. Haitjema, Y. Zhang, M. Vockenhuber, D. Kazazis, Y. Ekinci, A.M. Brouwer, Extreme ultraviolet patterning of tin-oxo cages, J. Micro/Nanolithogr MEMS MOEMS. 16 (2017) 1, https://doi.org/10.1117/1.jmm.16.3.033510.

[23] B. Cardineau, R. Del Re, M. Marnell, H. Al-Mashat, M. Vockenhuber, Y. Ekinci, C. Sarma, D.A. Freedman, R.L. Brainard, Photolithographic properties of tin-oxo clusters using extreme ultraviolet light (13.5 nm), Microelectron. Eng. 127 (2014) 44–50, https://doi.org/10.1016/j.mee.2014.04.024.

[24] A. Grenville, J.T. Anderson, B.L. Clark, P. De Schepper, J. Edson, M. Greer, K. Jiang, M. Kocsis, S.T. Meyers, J.K. Stowers, A.J. Telecky, D. De Simone, G. Vandenberghe, Integrated fab process for metal oxide EUV photoresist, Adv. Pattern. Mater. Process. XXXII. 9425 (2015) 94250S, https://doi.org/10.1117/12.2086006.

[25] S. Hasan, M. Murphy, M. Weires, S. Grzeskowiak, G. Denbeaux, R.L. Brainard, Oligomers of MORE: Molecular organometallic resists for EUV, in: R. Gronheid, D. P. Sanders (Eds.), Advances in Patterning Materials and Processes XXXVI, SPIE, 2019, p. 61, https://doi.org/10.1117/12.2516010.

[26] A.S. Gangnaik, Y.M. Georgiev, J.D. Holmes, New generation electron beam resists: a review, Chem. Mater. 29 (2017) 1898–1917, https://doi.org/10.1021/acs.chemmater.6b03483.

[27] D.R. Medeiros, A. Aviram, C.R. Guarnieri, W.-. Huang, R. Kwong, C.K. Magg, A. P. Mahorowala, W.M. Moreau, K.E. Petrillo, M. Angelopoulos, Recent progress in electron-beam resists for advanced mask-making, IBM J. Res. Dev. 45 (2001) 639–650, https://doi.org/10.1147/rd.455.0639.

[28] X. Thrun, K.-H. Choi, M. Freitag, A. Grenville, M. Gutsch, C. Hohle, J.K. Stowers, J. W. Bartha, Evaluation of direct patternable inorganic spin-on hard mask materials using electron beam lithography, Microelectron. Eng. 98 (2012) 226–229, https://doi.org/10.1016/j.mee.2012.07.017.

[29] D.X. Yang, A. Frommhold, A. McClelland, J. Roth, M. Rosamond, E.H. Linfield, J. Osmond, R.E. Palmer, A.P.G. Robinson, Performance of a high resolution chemically amplified electron beam resist at various beam energies, Microelectron. Eng. 155 (2016) 97–101, https://doi.org/10.1016/j.mee.2016.03.010.

[30] M. Sarkar, Y.N. Mohapatra, Electron beam lithography in thick negative tone chemically amplified resist: controlling sidewall profile in deep trenches and channels, Microelectron. Eng. 130 (2014) 1–7, https://doi.org/10.1016/j.mee.2014.08.006.

[31] H. Yang, A. Jin, Q. Luo, J. Li, C. Gu, Z. Cui, Electron beam lithography of HSQ/PMMA bilayer resists for negative tone lift-off process, Microelectron. Eng. 85 (2008) 814–817, https://doi.org/10.1016/j.mee.2008.01.006.

[32] M. Zhu, C. Mei, J. Deng, Y. Xie, Y. Chen, Evaluation of RE-650 as a positive tone resist for electron beam lithography with high plasma etch durability, Microelectron. Eng. 227 (2020), 111271, https://doi.org/10.1016/j.mee.2020.111271.

[33] A. Cattoni, D. Mailly, O. Dalstein, M. Faustini, G. Seniutinas, B. Rösner, C. David, Sub-10 nm electron and helium ion beam lithography using a recently developed alumina resist, Microelectron. Eng. 193 (2018) 18–22, https://doi.org/10.1016/j.mee.2018.02.015.

[34] S. Pfirrmann, A. Voigt, A. Kolander, G. Grützner, O. Lohse, I. Harder, V.A. Guzenko, Towards a novel positive tone resist mr-PosEBR for high resolution electron-beam lithography, Microelectron. Eng. 155 (2016) 67–73, https://doi.org/10.1016/j.mee.2016.02.028.

[35] R. Kirchner, V.A. Guzenko, I. Vartiainen, N. Chidambaram, H. Schift, ZEP520A - a resist for electron-beam grayscale lithography and thermal reflow, Microelectron. Eng. 153 (2016) 71–76, https://doi.org/10.1016/j.mee.2016.01.017.

[36] N. Tiwale, A. Subramanian, K. Kisslinger, M. Lu, J. Kim, A. Stein, C.-Y. Nam, Advancing next generation nanolithography with infiltration synthesis of hybrid nanocomposite resists, J. Mater. Chem. C 7 (2019) 8803–8812, https://doi.org/10.1039/C9TC02974E.

[37] V. Canalejas-Tejero, S. Carrasco, F. Navarro-Villoslada, J.L. García Fierro, M.D. C. Capel-Sánchez, M.C. Moreno-Bondi, C.A. Barrios, Ultrasensitive non-chemically amplified low-contrast negative electron beam lithography resist with dual-tone behaviour, J. Mater. Chem. C 1 (2013) 1392–1398, https://doi.org/10.1039/c2tc00148a.

[38] M. Gersborg-Hansen, L.H. Thamdrup, A. Mironov, A. Kristensen, Combined electron beam and UV lithography in SU-8, Microelectron. Eng. 84 (2007) 1058–1061, https://doi.org/10.1016/j.mee.2007.01.084.

[39] M. Aktary, M.O. Jensen, K.L. Westra, M.J. Brett, M.R. Freeman, High-resolution pattern generation using the epoxy novolak SU-8 2000 resist by electron beam lithography, J. Vacuum Sci. Technol. B: Microelectron Nanomet. Struct. 21 (2003) L5, https://doi.org/10.1116/1.1596216.

[40] I. Raptis, N. Glezos, E. Valamontes, E. Zervas, P. Argitis, Electron beam lithography simulation for high resolution and high-density patterns, Vacuum. 62 (2001) 263–271, https://doi.org/10.1016/S0042-207X(00)00448-6.

[41] X. Wang, W. Hu, R. Ramasubramaniam, G.H. Bernstein, G. Snider, M. Lieberman, Formation, characterization, and sub-50-nm patterning of organosilane monolayers with embedded disulfide bonds: An engineered self-assembled monolayer resist for electron-beam lithography, Langmuir. 19 (2003) 9748–9758, https://doi.org/10.1021/la035291e.

[42] G.K. Belmonte, S.W. Cendron, P. Guruprasad Reddy, C.A.S. Moura, M. Ghulam Moinuddin, J. Peter, S.K. Sharma, G. Albara Lando, M. Puiatti, K.E. Gonsalves, D. E. Weibel, Mechanistic insights of Sn-based non-chemically-amplified resists under EUV irradiation, Appl. Surf. Sci. 533 (2020), 146553, https://doi.org/10.1016/j.apsusc.2020.146553.

[43] K. Nozaki, E. Yano, New protective groups in alicyclic methacrylate polymers for 193-nm resists, J. Photopolym. Sci. Technol. 10 (1997) 545–550, https://doi.org/10.2494/photopolymer.10.545.

[44] B. Lei, J. Jiang, Y. Jia, L. Liu, W. Chang, J. Li, Novel organotin-containing diblock copolymer with tunable nanostructures: synthesis, self-assembly and morphological change, J. Organomet. Chem. 696 (2011) 1416–1424, https://doi.org/10.1016/j.jorganchem.2011.01.004.

[45] M. Wang, K.E. Gonsalves, W. Yueh, J.M. Roberts, Novel anionic Photoacid generators (PAGs) and corresponding PAG bound polymers, Macromol. Rapid Commun. 27 (2006) 1590–1595, https://doi.org/10.1002/marc.200600330.

[46] M. Wang, W. Yueh, K.E. Gonsalves, Fluorine-contained photoacid generators (PAGs) and corresponding polymer resists, J. Fluor. Chem. 129 (2008) 607–612, https://doi.org/10.1016/j.jfluchem.2008.04.014.

[47] M. Wang, M. Tang, T.-H. Her, W. Yueh, K.E. Gonsalves, Synthesis, characterization and lithography performance of novel anionic Photoacid generator (PAG) bound polymers, J. Photopolym. Sci. Technol. 20 (2007) 793–797, https://doi.org/10.2494/photopolymer.20.793.

[48] J. Peter, M.G. Moinuddin, S. Ghosh, S.K. Sharma, K.E. Gonsalves, Organotin in nonchemically amplified polymeric hybrid resist imparts better resolution with sensitivity for next-generation lithography, ACS Appl. Polym. Mater. 2 (2020) 1790–1799, https://doi.org/10.1021/acsapm.0c00005.

[49] R.J.H. Clark, A.G. Davies, R.J. Puddephatt, The infrared spectra (650–70 cm. –1) of alkyl tin halides and their adducts with 2,2′-bipyridyl and 1,10-phenanthroline, J. Chem. Soc. A (1968) 1828–1834, https://doi.org/10.1039/J19680001828.

[50] N. Mojarad, J. Gobrecht, Y. Ekinci, Beyond EUV lithography: a comparative study of efficient photoresists' performance, Sci. Rep. 5 (2015) 9235, https://doi.org/10.1038/srep09235.

[51] A. Robinson, R. Lawson, Materials and Processes for Next Generation Lithography, Elsevier Science, 2016.

[52] B. Bilenberg, S. Jacobsen, M.S. Schmidt, L.H.D. Skjolding, P. Shi, P. Bøggild, J. O. Tegenfeldt, A. Kristensen, High resolution 100 kV electron beam lithography in SU-8, Microelectron. Eng. 83 (2006) 1609–1612, https://doi.org/10.1016/j.mee.2006.01.142.

[53] M. Schirmer, B. Büttner, F. Syrowatka, G. Schmidt, T. Köpnick, C. Kaiser, Chemical semi-amplified positive E-beam resist (CSAR 62) for highest resolution, 29th European Mask and Lithography Conference 8886, 2013, p. 88860D, https://doi.org/10.1117/12.2030576.

[54] J. Saint-Pol, S. Landis, C. Gourgon, S. Tedesco, R. Hanawa, M. Suetsugu, M. Akita, S. Yamamoto, Negative tone chemically amplified resist formulation optimizations for ultra high-resolution lithography, Microelectron. Eng. 67–68 (2003) 274–282, https://doi.org/10.1016/S0167-9317(03)00186-2.

[55] H. Tsubaki, S. Tarutani, N. Inoue, H. Takizawa, T. Goto, EUV resist materials design for 15 nm half pitch and below, J. Photopolym. Sci. Technol. 26 (2013) 649–657.

[56] H. Duan, D. Winston, J.K.W. Yang, B.M. Cord, V.R. Manfrinato, K.K. Berggren, Sub-10-nm half-pitch electron-beam lithography by using poly(methyl methacrylate) as a negative resist, J. Vacuum Sci. Technol. B, Nanotechnol. Microelectronics: Mater. Process. Measur. Phenomena. 28 (2010), https://doi.org/10.1116/1.3501353. C6C58-C6C62.

[57] S. Yasin, D.G. Hasko, H. Ahmed, Fabrication of <5 nm width lines in poly (methylmethacrylate) resist using a water:isopropyl alcohol developer and ultrasonically-assisted development, Appl. Phys. Lett. 78 (2001) 2760–2762, https://doi.org/10.1063/1.1369615.

[58] J.K.W. Yang, B. Cord, H. Duan, K.K. Berggren, J. Klingfus, S.-W. Nam, K.-B. Kim, M. J. Rooks, Understanding of hydrogen silsesquioxane electron resist for sub-5-nm-half-pitch lithography, J. Vacuum Sci. Technol. B: Microelectron Nanomet. Struct. 27 (2009) 2622, https://doi.org/10.1116/1.3253652.

[59] J. Reinspach, M. Lindblom, O. von Hofsten, M. Bertilson, H.M. Hertz, A. Holmberg, Cold-developed electron-beam-patterned ZEP 7000 for fabrication of 13 nm nickel zone plates, J. Vacuum Sci. Technol. B: Microelectron Nanomet. Struct. 27 (2009) 2593, https://doi.org/10.1116/1.3237140.

[60] L.Y.M. Tobing, L. Tjahjana, D.H. Zhang, Direct patterning of high density sub-15 nm gold dot arrays using ultrahigh contrast electron beam lithography process on positive tone resist, Nanotechnology. 24 (2013) 75303, https://doi.org/10.1088/0957-4484/24/7/075303.

[61] J. Peter, M.G. Moinuddin, S. Ghosh, S.K. Sharma, K.E. Gonsalves, Organotin in nonchemically amplified polymeric hybrid resist imparts better resolution with sensitivity for next-generation lithography, ACS Appl. Polym. Mater. 2 (2020) 1790–1799, https://doi.org/10.1021/acsapm.0c00005.

[62] A. Gangnaik, Y.M. Georgiev, B. McCarthy, N. Petkov, V. Djara, J.D. Holmes, Characterisation of a novel electron beam lithography resist, SML and its comparison to PMMA and ZEP resists, Microelectron. Eng. 123 (2014) 126–130, https://doi.org/10.1016/j.mee.2014.06.013.

[63] K.C. Fairley, M.C. Sharps, G. Mitchson, J. Ditto, D.W. Johnson, D.C. Johnson, Sub-30 keV patterning of HafSOx resist: effects of voltage on resolution, contrast, and sensitivity, J. Vacuum Sci. Technol. B, Nanotechnol. Microelectronics: Mater. Process. Measur. Phenomena. 34 (2016), 041607, https://doi.org/10.1116/1.4954394.

[64] J. Stowers, D.A. Keszler, High resolution, high sensitivity inorganic resists, Microelectron. Eng. 86 (2009) 730–733, https://doi.org/10.1016/j.mee.2008.11.034.

[65] J. Kofler, K. Schmoltner, A. Klug, E.J.W. List-Kratochvil, Highly robust electron beam lithography lift-off process using chemically amplified positive tone resist and PEDOT:PSS as a protective coating, J. Micromech. Microeng. 24 (2014) 95010, https://doi.org/10.1088/0960-1317/24/9/095010.

[66] H. Okamura, D.C. Forman, C.K. Ober, C60-containing polymers for electron beam lithography, Polym. Bull. 71 (2014) 2395–2405, https://doi.org/10.1007/s00289-014-1197-z.
[67] D.X. Yang, A. Frommhold, X. Xue, R.E. Palmer, A.P.G. Robinson, Chemically amplified phenolic fullerene electron beam resist, J. Mater. Chem. C 2 (2014) 1505–1512, https://doi.org/10.1039/c3tc31896f.
[68] S. Pfirrmann, R. Kirchner, O. Lohse, V.A. Guzenko, A. Voigt, I. Harder, A. Kolander, H. Schift, G. Grützner, Mr-PosEBR: a novel positive tone resist for high resolution electron beam lithography and 3D surface patterning, Adv. Pattern. Mater. Processes XXXIII. 9779 (2016), 977925, https://doi.org/10.1117/12.2219165.
[69] A.S. Abbas, S. Alqarni, B.B. Shokouhi, M. Yavuz, B. Cui, Water soluble and metal-containing electron beam resist poly (sodium 4-styrenesulfonate), Mater. Res. Express. 1 (2014) 45102, https://doi.org/10.1088/2053-1591/1/4/045102.
[70] M.S.M. Saifullah, M. Asbahi, M. Binti-Kamran Kiyani, S.S. Liow, S. Bin Dolmanan, A.M. Yong, E.A.H. Ong, A. Ibn Saifullah, H.R. Tan, N. Dwivedi, T. Dutta, R. Ganesan, S. Valiyaveettil, K.S.L. Chong, S. Tripathy, Room-temperature patterning of nanoscale MoS2 under an Electron beam, ACS Appl. Mater. Interfaces 12 (2020) 16772–16781, https://doi.org/10.1021/acsami.9b22229.
[71] M.S.M. Saifullah, M. Asbahi, M. Binti-Kamran Kiyani, S. Tripathy, E.A.H. Ong, A. Ibn Saifullah, H.R. Tan, T. Dutta, R. Ganesan, S. Valiyaveettil, K.S.L. Chong, Direct patterning of zinc sulfide on a Sub-10 nanometer scale via Electron beam lithography, ACS Nano 11 (2017) 9920–9929, https://doi.org/10.1021/acsnano.7b03951.
[72] S. Kim, B. Marelli, M.A. Brenckle, A.N. Mitropoulos, E.S. Gil, K. Tsioris, H. Tao, D. L. Kaplan, F.G. Omenetto, All-water-based electron-beam lithography using silk as a resist, Nat. Nanotechnol. 9 (2014), https://doi.org/10.1038/nnano.2014.47.
[73] Q. Wang, C. Zhang, C. Yan, F. You, L. Wang, One-component chemically amplified resist composed of polymeric sulfonium salt PAGs for high resolution patterning, Eur. Polym. J. 114 (2019) 11–18, https://doi.org/10.1016/j.eurpolymj.2019.01.064.
[74] I. Haller, Electron impact reactions of triphenylsulfonium salt resist sensitizers in the solid state, J. Vacuum Sci. Technol. B: Microelectron Nanomet. Struct. 9 (1991), https://doi.org/10.1116/1.585343.
[75] T. Kozawa, S. Tagawa, H.B. Cao, H. Deng, M.J. Leeson, Acid distribution in chemically amplified extreme ultraviolet resist, J. Vacuum Sci. Technol. B: Microelectron Nanomet. Struct. 25 (2007), https://doi.org/10.1116/1.2794063.
[76] V. Spampinato, A. Franquet, D. de Simone, I. Pollentier, A. Pirkl, H. Oka, P. van der Heide, SIMS analysis of thin EUV photoresist films, Anal. Chem. 94 (2022) 2408–2415, https://doi.org/10.1021/acs.analchem.1c04012.